Available online at www.sciencedirect.com
SCIENCE DIRECT
Journal of Molecular Catalysis A: Chemical 255 (2006) 36–40
JOURNAL OF MOLECULAR CATALYSIS A: CHEMICAL
www.elsevier.com/locate/molcata

Effect of preparation parameters on the properties of $La_{0.9}Ce_{0.1}CoO_3$ catalysts: An EMR investigation

C. Oliva [a,*], S. Cappelli [a], A. Kryukov [b], G.L. Chiarello [a], A.V. Vishniakov [b], L. Forni [a]

[a] *Dipartimento di Chimica Fisica ed Elettrochimica, Università degli Studi di Milano, CNR Institute, via C.Golgi, 1920133 Milano, Italy*
[b] *D.I.Mendeleev Chemical-Technological University of Russia, Moscow, Russia*

Received 3 February 2006; received in revised form 24 March 2006; accepted 28 March 2006
Available online 3 May 2006

Abstract

A few $La_{1-x}Ce_xCoO_3$ ($x = 0$; 0.1) catalysts, prepared by the traditional sol–gel (SG) or by flame pyrolysis (FP) procedures have been analysed by EPR spectroscopy at $120 \leq T \leq 300$ K. No EPR line was noticed with all of the $x = 0$ samples. The $x = 0.1$ SG catalysts gave a single EPR feature at $g \cong 2$, both when fresh and after catalytic reaction. This line was Lorentzian shaped at 120 K, broadening with increasing temperature, and also becoming a bit asymmetric after catalytic use. The $x = 0.1$ FP samples gave an EPR spectrum only after catalytic reaction. This pattern was rather similar to that obtained with the fresh SG sample with the same composition, but shifted towards lower magnetic field values. Furthermore, all the FP samples showed an intense ferromagnetic signal (FMR) after degassing treatment, while they remained EPR silent after oxygenation. An interpretation of most of these observations is here proposed on the base of *polaron* propagation and of formation of ferromagnetic *spin bags*. A correlation between catalytic performance, XRD patterns and electron magnetic resonance (EMR) (i.e. EPR or FMR) spectra, has been also highlighted.

Keywords: Perovskites; Methane flameless combustion; EPR analysis

1. Introduction

Perovskitic samples of formula $La_{1-x}Ce_xCoO_3$ are well known as quite active catalysts for exhaust gas depollution [1,2] as well as for the catalytic flameless combustion (CFC) of methane [3,4]. Indeed, samples of this kind, prepared by the traditional sol–gel (SG) procedure have been successfully tested for CO oxidation with air [1] and NO reduction by CO [2]. In the last case, after reaction the samples showed a Lorentzian-shaped EPR line, linearly broadening with temperature. This was attributed to spin–spin superexchange, occurring between nearest neighbour Co paramagnetic ions through oxygen-based bridges. The temperature-dependent line broadening was then attributed to polaron propagation, i.e to spin–phonon interactions. Similar Lorentzian-shaped lines were observed also with $La_{1-x}Ce_xCoO_3$ prepared by SG from oxide mixtures in molten ammonium nitrate or citrate ("A" and "C" samples, respectively) [4]. However, in that case some samples showed the Lorentzian line both when fresh and after CFC of methane; some other, among which the best catalyst (i.e. the $x = 0.2$ sample of the "C" series), showed that line only after catalytic reaction. Furthermore, only the fresh samples with $x = 0.1$ of both "A" and "C" series showed a broad intense absorption at magnetic field values lower than 2000 G, attributed to ferromagnetic resonance (FMR) of domains perhaps involving O_{ads}^- "spin bags" and Co magnetic ions.

However, $La_{1-x}Ce_xCoO_3$ samples prepared by a different method (flame-hydrolysis, FH) and employed in the same CFC of methane, did show any of the above mentioned EPR or FMR spectra neither when fresh, nor after reaction, though being by far better catalysts than those above mentioned [3].

Aiming at a better understanding of this very complicate situation, in the present investigation we prepared a few $La_{1-x}Ce_xCoO_3$ samples ($x = 0$; 0.1) following the traditional SG method or a different recently proposed procedure, based on a flame pyrolysis (FP) treatment [5]. These catalysts have been analysed by XRD, EPR and BET, before and after use in the

* Corresponding author. Tel.: +39 02 50314270; fax: +39 02 50314300.
E-mail address: cesare.oliva@unimi.it (C. Oliva).

1381-1169/$ – see front matter © 2006 Elsevier B.V. All rights reserved.
doi:10.1016/j.molcata.2006.03.065

CFC of methane, looking for correlations between preparation parameters and sample structural and physical–chemical properties, including of course catalytic activity.

2. Experimental

2.1. Materials

$La_{1-x}Ce_xCoO_3$ ($x = 0$; 0.1) loose powder samples have been prepared by the SG procedure [6] from La, Ce, Co acetates solution containing an equimolar amount of citric acid and calcined at 800 °C for 8 h (SG0 and SG1 samples, respectively). (FP0) samples with $x = 0$ have been prepared by FP, starting from a 1:1 fuel mixture of propionic acid and *n*-octanol or ethanol containing the proper amount of the three metal acetates in stoichiometric ratio, obtaining identical results in the two cases. (FP1) samples with $x = 0.1$ have been prepared by FP, starting from the same metal acetates dissolved in a 1:1 mixture of propionic acid and propanol. A further (FP1P) sample of the last kind has been prepared by the same procedure, but adding 0.25 wt% of Pt and 0.75 wt% of Pd.

2.2. Catalyst characterization

EPR spectra have been collected by means of a Bruker Elexsys spectrometer at the working frequency of 9.4 GHz and temperature generally ranging between 120 and 300 K, on fresh catalysts or after catalytic use (U-labelled samples in figure captions) for the CFC of methane. The catalytic activity was measured by loading 0.2 g of catalyst, diluted with 1.3 g of quartz powder of the same particle size (60–100 mesh) in a continuous tubular microreactor, to which a mixture of 20 $cm^3\ min^{-1}$ of a 1 vol% CH_4 in N_2 + 20 $cm^3\ min^{-1}$ of air was fed, while increasing temperature by 2 K min^{-1} up to 873 K.

XRD patterns have been collected by means of a Philips PW1820 powder diffractometer by employing the Ni-filtered Cu Kα radiation ($\lambda = 0.15148$ nm). The solid phases have been recognised by comparison with literature data [7(a)].

3. Results

3.1. XRD analysis

XRD analysis showed that SG0 and FP0 possessed an identical, perovskite-like structure. This was not always the case when 10% Ce substituted for La. Indeed, FP1 sample preserved its perovskite-like structure (Fig. 1(a)), while small amounts of Co_3O_4 and CeO_2 phases formed in SG1, producing a structure (Fig. 1(c)) more similar to that acquired by FP1 after catalytic reaction (FP1U sample, Fig. 1(b)).

3.2. EPR spectra

No EPR signal has been obtained with all the $x = 0$ samples, i.e. with SG0 and FP0 catalysts, either when fresh, or after their use for the CFC of methane. On the contrary, the SG1 sample gave a single EPR feature with $g \cong 2$, both when

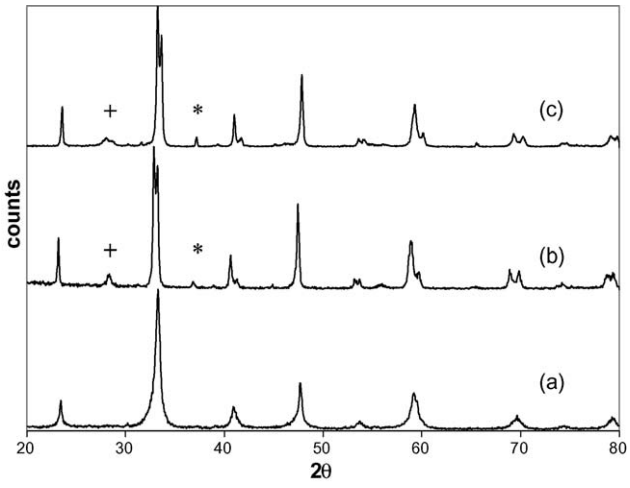

Fig. 1. XRD patterns of $La_{0.9}Ce_{0.1}CoO_3$: (a) FP1, (b) FP1U, (c) SG1. (*) Co_3O_4; (+) CeO_2 phases.

fresh (SG1, Fig. 2(a)) and after CFC of methane (SG1U, Fig. 2(b)), broadening with increasing temperature and keeping a Lorentzian shape up to 190 K. Furthermore, the line of SG1 retained almost perfectly its shape also at $T \geq 200$ K, with a temperature-independent $g \cong 2.23$ value. By contrast, the line of SG1U kept the Lorentzian shape and a constant value of $g \cong 2.28$ for 120 K $\leq T \leq$ 190 K only, whereas g increased up to ≅2.44 and the spectral shape became asymmetric when temperature increased up to 330 K. The double integrated intensity increased markedly at lower temperature with SG1, whereas it remained nearly unchanged with SG1U (Fig. 3).

The FP1 and FP1P samples behaved in a different way. In fact, no EMR signal was observed with them when fresh, whereas they showed an asymmetric EMR pattern after CFC of methane, at field values ranging between 0 and ca. 6000 G and with broad low-field peaks. The intensity of this low-field portion of the spectrum decreases at higher temperature. In particular, the spectrum transformed into a nearly Lorentzian-shaped line at $T \geq 200$ K, with an apparent g value decreasing from 2.74 down to 2.69 and a peak-to-peak line-width decreasing from 1850 down to 1600 G, when the temperature increased from 200 (Fig. 2(c)) up to 290 K. Amounts of the (EPR silent) FP0 and FP1P samples were subjected to an oxidation or a degassing treatment. No EPR spectrum was observed after the former process. On the contrary, degassing led to an intense low-field

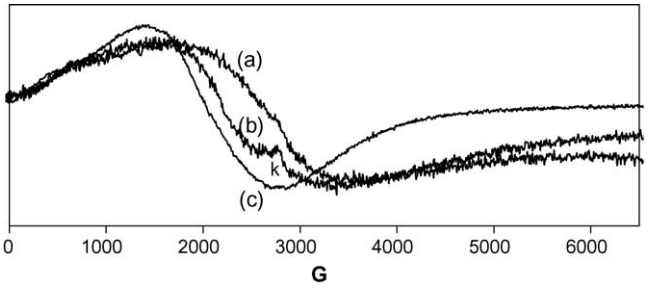

Fig. 2. EPR spectra at 200 K of $La_{0.9}Ce_{0.1}CoO_3$ samples: (a) SG1, (b) SG1U, (c) FP1U. The bump *k* is due to the instrument cavity, and not to the sample. Multiplication factor 3 for the intensity of the (a and b) tracks.

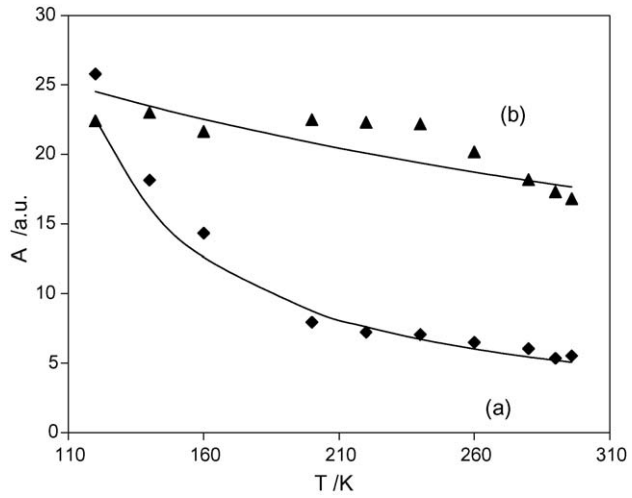

Fig. 3. Double integrated intensity A (arbitrary units) of the EMR spectra obtained (a) with SG1 and (b) with SG1U sample. The best-fitting lines are (a) A(SG1) = 1149/(T − 68.94) and (b) A(SG1U) = 11111/(T + 333.33) (statistical error on the last digit of the fitting parameters).

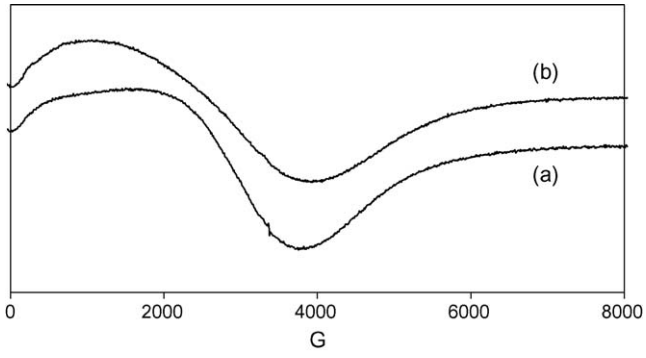

Fig. 4. FMR patterns after degassing (a) $LaCoO_3$ (FP0) and (b) $La_{0.9}Ce_{0.1}CoO_3$ (FP1P) samples. Recording temperature: 290 K.

absorption signal (Fig. 4) with temperature-dependent shape. Its intensity decreased by ca. 25% when increasing temperature from 120 up to 290 K. No reliable double integrated intensity values could be obtained from these patterns, due to their broadness and irregular shape.

4. Discussion

4.1. $g \cong 2$ EPR line and sample preparation parameters

When Lorentzian-shaped, the SG1 and SG1U EPR feature (Fig. 2(a and b)) is similar to that already reported [4] for $La_{1-x}Ce_xCoO_3$ ($x = 0.05$, 0.2), prepared from oxide mixtures in molten ammonium nitrate (thereafter referred to as A05 and A2 samples, respectively), and with $x = 0.05$, prepared by the same technique, but from ammonium citrate (thereafter referred to as C05 sample). However, no EPR line of this kind was noted with A1 and C1, i.e. with samples prepared by the same methods followed for A05 and C05, respectively, but with $x = 0.1$ as for SG1. Therefore, the properties of $La_{1-x}Ce_xCoO_3$ catalysts seem extremely sensitive to the preparation parameters and rather different materials can be obtained with the same nominal composition. In particular, the CeO_2 and/or Co_3O_4 phases noticed with SG1 (Fig. 1(c)), accompanied by La_2O_3, were reported also with the above mentioned $La_{1-x}Ce_xCoO_3$ "A" and "C" samples [4]. In our opinion, these phases can form through decomposition reactions like:

$$120\,La_{0.9}Ce_{0.1}CoO_{3+\delta} \rightarrow 12\,CeO_2 + 54\,La_2O_3 + 40\,Co_3O_4 + 7\,O_2 \quad (1)$$

where $\delta = 0.05$ to obtain charge neutrality in the example of Eq. (1), i.e. when $x = 0.1$.

The present preparation was carried out under O_2-rich atmosphere. This accounts for the fact that no CoO phase [7(b)] forms. Indeed, Co^{3+} and hence O-richer oxides, like Co_3O_4 [7(c)] and $LaCoO_3$, are favoured. Then, the transformation of Co_3O_4 into CoO, though thermodynamically favoured, does not occur, due to kinetic reasons, i.e. to the rapid quenching of the particles after their formation in the flame. Furthermore, the presence of traces of the right-hand phases in Eq. (1) suggests the formation also of the other products, though frequently not detectable by XRD analysis. Hence, it seemed difficult to correlate the presence of these decomposition products to that of the Lorentzian-shaped line only on the base of the results reported in ref. [4]. However, the XRD patterns indicate that solids prepared by FH [3] or by FP (Fig. 1(a)) possess a perfect perovskitic structure, though the last is not thermodynamically favoured with respect to other Co oxidic species. On the other hand, the perovskitic phase is the most stable one at temperatures as high as those attained in the FH and FP procedures. These FH and FP solids do not show any Lorentzian EPR line at $g \cong 2$. The same situation has been observed by us also with $La_{0.9}M_{0.1}CoO_3$ (M = Pr, Sm, Tb) samples prepared by FP and analysed both before and after CFC of methane [8]. Furthermore, in the present investigation, we have observed that Co_3O_4 and CeO_2 phases appear in the FP1 sample, but only after the CFC of methane (sample FP1U), so that its structure (Fig. 1(b)) becomes similar to that of the fresh SG1 sample (Fig. 1(c)). As a consequence, a Lorentzian-shaped line appears also in the EPR spectrum of FP1U (Fig. 2(c)). We can conclude that pure mono-phasic perovskite-like $La_{1-x}Ce_xCoO_3$ samples do not show any $g \cong 2$ Lorentzian-shaped line, as with FP1 and the samples prepared by the FH method [3]. Such a line can appear with these samples after catalytic reaction only, when sufficient amounts of La_2O_3, CeO_2 and/or Co_3O_4 phases form. Therefore, in general we can say that in the presence of monometallic phases a $g \cong 2$ Lorentzian-shaped line appears, though in a very few cases this does not occur, as observed with the C1 and C2 SG samples [4].

4.2. $g \cong 2$ EPR line and sample catalytic activity

$La_{1-x}Ce_xCoO_3$ ($x = 0$; 0.1) samples prepared by FP in the present investigation, as well as those prepared by FH [3], are by far better catalysts than those prepared by SG, like SG1 (Fig. 5) and those of "A" and "C" series of ref. [4].

The FH and FP samples possess a pure perovskite-like structure, while those prepared by SG usually undergo the decomposition reaction (1), at least in part, leading to La_2O_3, CeO_2

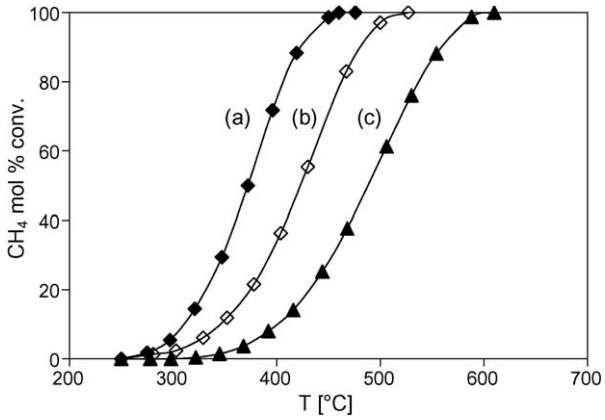

Fig. 5. Activity of $La_{0.9}Ce_{0.1}CoO_3$ for CFC of methane (a) fresh FP1; (b) FP1 after three deactivation cycles (activity decreases significantly only after the first cycle; (c) SG1: activity curves are identical with fresh sample and after three deactivation cycles.

and/or Co_3O_4 phases formation. As a consequence, SG-prepared samples generally show the Lorentzian-shaped $g \cong 2$ EPR line. However, as above-mentioned, this line does not appear with C1 and C2, which are the best catalysts of the "C" series. On the other hand, reactions like (1) would provide $O_{2(g)}$ to the catalytic reaction if occurring at a sufficiently high temperature only. On the contrary, samples undergoing the decomposition (1) at a too low temperature would be bad catalysts.

Therefore, we can conclude that good $La_{1-x}Ce_xCoO_3$ catalysts are characterised by pure perovskitic structure (without other phases like CeO_2, La_2O_3 or Co_3O_4) and by the absence of the $g \cong 2$ EPR line.

4.3. The origin of the EPR $g \cong 2$ line

Generallly the $3d^6$ Co^{3+} ions are stable in the low spin ($S = 0, t_{2g}^6, e_g^0$) state when octahedrally coordinated to six oxygen atoms in an ideal $LaCoO_3$ structure [9]. Ions of this kind can also form oxygen-based species such as Co^{3+}/O_2^- pairs [2,10,11]. Species like these could contribute to the asymmetric EPR pattern at room temperature, here reported, which are masked at lower temperatures by the more intense Lorentzian-shaped line.

A $g \cong 2$ Lorentzian-shaped line, broadening with increasing temperature, has been noticed since a long time also with Co_3O_4 [12–14]. Narrower lines were obtained with this solid at higher preparation temperature, i.e. at lower residual disorder. The magnetic structure of this cobalt oxide has been deeply investigated [14]. Units like:

$$- O^{2-} - Co^{3+} - O^{2-} - \underline{Co^{2+} - O^{2-} - Co^{3+} - O^{2-} - Co^{2+}} - O^{2-} -$$

Scheme 1

have been hypothesised, in which two Co^{2+} ($3d^7$, $S = 3/2$) ions, localised in tetrahedral sites, would interact with each other through O^{2-}–Co^{3+}–O^{2-} bridges, Co^{3+} ($3d^6$, $S = 0$) being localised in octahedral field. Two sets of units like that outlined in Scheme 1 would form, characterised by antiferromagnetic (AFM) and ferromagnetic (FM) coupling, respectively. The former would have multiplicity 12, the latter multiplicity 24. Other similar schemes have been elsewhere proposed [12,13]. In any case, also the fitting parameters reported in the caption of Fig. 3 suggest a prevailing of FM over AFM interactions in SG1. By contrast, AFM interactions would prevail with SG1U, i.e. after catalytic reaction, probably because the catalyst chemical reduction transforms some Co^{3+} into Co^{2+} ions, directly interacting with each other by AFM superexchange through an O^{2-} ion. However, only these qualitative considerations can be advanced, because of the error affecting the values of the double integrated intensities of these broad experimental lines. Analogous interpretations can account also for the observed Lorentzian-shaped line reported in the above-mentioned cases with $La_{1-x}Ce_xCoO_3$ samples. Indeed, we have above outlined that in many cases XRD patterns reveal the presence of extraneous phases, including Co_3O_4, in $La_{1-x}Ce_xCoO_3$ samples, depending on the preparation parameters. On the other hand, the presence of Co_3O_4 in the fresh sample indicates that reaction (1) has already occurred and, therefore, that the sample has already lost a part of its oxygen. As a consequence, the presence of the Lorentzian-shaped line at $g \cong 2$ in a fresh sample indicates a bad catalyst (as here with SG1, as well as with samples of the "A" series in ref. [4]), while the appearance of this line after reaction indicates that the catalyst loosed a part of its oxygen through reaction (1) (as here with FP1U, as well as in ref. [2] and with C0 and C2 samples in ref. [4]). The FM interactions appeared uniformly distributed throughout all the SG1 sample, because no significant g shift was detected with increasing T, so excluding the formation of temperature-dependent FM domains. However, the situation changed at $T \geq 200$ K after catalytic reaction. Indeed, the apparent value of g increased with SG1U at these temperatures, indicating that some internal field was arising in the sample, presumably due to formation of FM domains. This interpretation is in line also with the asymmetric shape assumed at these temperatures by the EMR line of SG1U, attributable to some FMR contribution (vide infra).

4.4. The origin of the FMR at low magnetic field

The low-field absorption recorded with FP0 and FP1P samples after the degassing treatment (Fig. 4), i.e. after chemical reduction, can be attributed to the formation of FM domains large enough to give a FMR spectrum. Similar spectra were observed with A1 and C1 samples [4], as well as with $La_{1-x}Sr_xCoO_3$ ($x = 0.1$) [15] and with other perovskitic [16–18] and fluoritic [8,19] materials. In those cases, an explanation was proposed, involving the formation of FM domains, composed of O_{ads}^- ions interacting with each other and possibly with other paramagnetic ions. Alternatively, the formation of ferromagnetic metallic clusters of Co^{4+} only has been invoked in a more recent paper [20] to explain this low-field broad absorption band when Ca^{2+} or Sr^{2+} substitute for La^{3+}.

The formation of O_{ads}^- was hypothesised in ref. [15] as a consequence of oxygen vacancies $V_O^{\bullet\bullet}$ created through the substitution of Sr^{2+} for La^{3+}. Oxygen vacancies can be created also

in the present case by substituting Ce^{4+} for La^{3+}. Indeed, the following reaction can occur:

$$Ce^{4+}O_2{}^{2-} \rightarrow Ce_{La}{}^{\bullet} + 2O_i{}^{2-} + h^{\bullet} + V_O{}^{\bullet\bullet} \quad (2)$$

Here dots indicate the equivalence of introducing positive charges into the system.

$Ce_{La}{}^{\bullet}$ is the defect formed by substituting Ce^{4+} for La^{3+}, $h^{\bullet}$ is an electron vacancy, as a Co ion in a high oxidation state. During the sample oxidation process, about a half of the interstitial oxygen $O_i{}^{2-}$ can react with $V_O{}^{\bullet\bullet}$, forming reticular oxygen $O_o{}^{x}$:

$$Ce_{La}{}^{\bullet} + 2O_i{}^{2-} + h^{\bullet} + V_O{}^{\bullet\bullet} \rightarrow Ce_{La}{}^{\bullet} + O_i{}^{2-} + O_o{}^{x} + h^{\bullet} \quad (3)$$

when the oxidised samples are degassed, the following process can occur [4]:

$$Ce_{La}{}^{\bullet} + O_i{}^{2-} + O_o{}^{x} + h^{\bullet} \rightarrow Ce_{La}{}^{\bullet} + O_i{}^{2-} + O_{ads}{}^{-} + V_O{}^{\bullet\bullet} \quad (4)$$

then, a few $O_{ads}{}^{-}$ ions could transform into $O_{2(g)}$ by donating their electron to some residual $h^{\bullet}$ (e.g. to some Co^{4+} ions), following the process:

$$2O_{ads}{}^{-} \leftrightarrow O_{2,ads}{}^{2-} \quad (5)$$

$$O_{2,ads}{}^{-} + h^{\bullet} \leftrightarrow O_{2,ads}{}^{2-} \quad (6)$$

$$O_{2,ads}{}^{-} + h^{\bullet} \leftrightarrow O_{2,g} \quad (7)$$

However, TPD analysis [3] showed that only very small amounts of pre-adsorbed oxygen desorb at room temperature from samples of this kind. Furthermore, most of $h^{\bullet}$ have been chemically reduced during the degassing process (6)–(7). However, it is well known [21–23] that among the $O_{ads}{}^{-}$ species the magnetic attraction can overcome the electrostatic repulsion in the proximity of positive charges, such as those present in these samples. Therefore, if reactions (5)–(7) do not occur, $O_{ads}{}^{-}$ are allowed to group into FM *spin bags* within internal cavities, where they cannot react with adsorbed substrates, causing the intensive FMR line shown in Fig. 4, as already proposed in refs. [4,15,19]. Furthermore, their presence could cause an internal magnetic field, able to account for the spectral shift towards lower magnetic field values observed with the used samples (compare Fig. 2(b and c) with Fig. 2(a)).

5. Conclusions

Different preparation processes can lead to $La_{1-x}Ce_xCoO_3$ samples with the same nominal composition, but with very different physical–chemical properties, including catalytic activity. In particular, samples containing traces of La_2O_3, CeO_2 and Co_3O_4 are usually present in the samples obtained by the traditional SG process, while monophasic perovskite-like $La_{1-x}Ce_xCoO_3$ samples are produced through the more recently proposed high-temperature procedures, like FH and FP. SG samples typically show a $g \cong 2$ Lorentzian-shaped line, broadening with temperature, probably due to the presence of Co_3O_4 or similar systems with Co ions in different oxidation states. Only the high-performing catalysts of this kind do not show such an EPR line. By contrast, FH and FP samples, which are always better-performing catalysts than the SG ones, never show this line when fresh, sometimes showing it after catalytic reaction, accompanied by the appearance of the La_2O_3, CeO_2 and Co_3O_4 phases. Therefore, the appearance of this Lorentzian-shaped line indicates a low-performance or a used catalyst. Furthermore, in a few cases a broad microwave absorption feature appears in the low magnetic field spectral region with FP samples after a degassing treatment. This has been reported elsewhere also with some fresh SG samples. Such a pattern can be attributed to formation of ferromagnetic spin bags, mainly formed of $O_{ads}{}^{-}$ ions clustering in the presence of oxygen vacancies.

References

[1] L. Forni, C. Oliva, F.P. Vatti, M.A. Kandala, A.M. Ezerets, A.V. Vishniakov, Appl. Catal. B: Environ. 7 (1996) 269.
[2] L. Forni, C. Oliva, T. Barzetti, E. Selli, A.M. Ezerets, A.V. Vishniakov, Appl. Catal. B: Environ. 13 (1997) 35.
[3] R. Leanza, I. Rossetti, L. Fabbrini, C. Oliva, L. Forni, Appl. Catal. B: Environ. 28 (2000) 55.
[4] C. Oliva, L. Forni, A. D'Ambrosio, F. Navarrini, A.D. Stepanov, Z.D. Kagramanov, A.I. Mikhailichenko, Appl. Catal. A: Gen. 205 (2001) 245.
[5] G.L. Chiarello, I. Rossetti, L. Forni, J. Catal. 236 (2005) 251.
[6] M.S.G. Baythoun, F.R. Sale, J. Mater. Sci. 17 (1982) 2757.
[7] Selected powder diffraction data, Miner. DBM (1–40) JCPDS, Swarthmore, PA, (a) 1974–1982; (b) 43–1004; (c) 42–1467.
[8] C. Oliva, S. Cappelli, A. Kryukov, G.L. Chiarello, A.V. Vishniakov, L. Forni, J. Mol. Catal. A: Chem. 247 (2006) 248.
[9] A. Abragam, B. Bleaney, Electron Paramagnetic Resonance of Transition Ions, Dover, New York, 1986 (Chapters 9 and 10).
[10] D. Cordischi, V. Indovina, M. Occhiuzzi, A. Arieti, J. Chem. Soc. Faraday Trans. I 75 (1979) 533.
[11] E. Giamello, Z. Sojka, M. Che, A. Zecchina, J. Phys. Chem. 90 (1986) 6084.
[12] S. Angelov, E. Zhecheva, R. Stoyanova, M. Atanasov, J. Phys. Chem. Solids 51 (1990) 1157.
[13] C. Oliva, L. Forni, L. Formaro, Appl. Spectrosc. 50 (1996) 1395.
[14] W.L. Roth, J. Phys. Chem. Solids 25 (1964) 1.
[15] C. Oliva, L. Forni, A.V. Vishniakov, Spectrochim. Acta A 56 (2000) 301.
[16] C. Oliva, L. Forni, P. Pasqualin, A. D'Ambrosio, A.V. Vishniakov, Phys. Chem. Chem. Phys. 1 (1999) 335.
[17] A.I. Shames, E. Rozenberg, V. Markocich, M. Auslender, A. Yakubovsky, A. Maignan, C. Martin, B. Raveau, G. Gorodetsky, Solid State Commun. 126 (2003) 395.
[18] C. Oliva, S. Cappelli, I. Rossetti, A. Kryukov, L. Bonoldi, L. Forni, J. Mol. Catal. A: Chem 245 (2006) 55.
[19] C. Oliva, L. Forni, A.V. Vishniakov, Appl. Magn. Reson. 14 (1998) 283.
[20] P. Aleshkeyvych, M. Baran, S.N. Barilo, J. Fink-Finowicki, H. Szymczak, J. Phys.: Condens. Matter 16 (2004) L179.
[21] H. Thomann, R.A. Klemm, D.C. Johnston, P.J. Tindall, H. Jin, D.P. Goshorn, Phys. Rev. B 39 (1988) 6552.
[22] R.A. Klemm, H. Thomann, D.C. Johnston, Phys. Rev. B 37 (1988) 2239.
[23] K.C. Hass, in: H. Ehrenreich, T. Turnbull (Eds.), Solid State Physics, vol. 32, Academic Press, New York, 1989, p. 237.